Bioorganic & Medicinal Chemistry Letters 23 (2013) 791–796

Contents lists available at SciVerse ScienceDirect

Bioorganic & Medicinal Chemistry Letters

journal homepage: www.elsevier.com/locate/bmcl

Discovery of liver-targeted inhibitors of stearoyl-CoA desaturase (SCD1)

Yongqi Deng [a,*], Zhiwei Yang [a,†], Gerald W. Shipps Jr. [a,‡], Sie-Mun Lo [a], Robert West [b], Joyce Hwa [c], Shuqin Zheng [c], Constance Farley [b], Jean Lachowicz [b,§], Margaret van Heek [c], Alan S. Bass [b], Dinesh P. Sinha [b], Craig R. Mahon [c], Mark E. Cartwright [b]

[a] Merck Research Laboratories, 320 Bent Street, Cambridge, MA 02141, United States
[b] Merck Research Laboratories, 2015 Galloping Hill Road, Kenilworth, NJ 07033, United States
[c] Merck Research Laboratories, RY 80Y-215 126 E. Lincoln Avenue, Rahway, NJ 07065-0900, United States

ARTICLE INFO

Article history:
Received 25 September 2012
Revised 16 November 2012
Accepted 20 November 2012
Available online 5 December 2012

Keywords:
Stearoyl-coenzyme A desaturase 1
Spirocyclic oxazepine
Liver-targeted inhibitors
Saturated fatty acids
Unsaturated fatty acids

ABSTRACT

Inhibitors based on a benzo-fused spirocyclic oxazepine scaffold were discovered for stearoyl-coenzyme A (CoA) desaturase 1 (SCD1) and subsequently optimized to potent compounds with favorable pharmacokinetic profiles and in vivo efficacy in reducing the desaturation index in a mouse model. Initial optimization revealed potency preferences for the oxazepine core and benzylic positions, while substituents on the piperidine portions were more tolerant and allowed for tuning of potency and PK properties. After preparation and testing of a range of functional groups on the piperidine nitrogen, three classes of analogs were identified with single digit nanomolar potency: glycine amides, heterocycle-linked amides, and thiazoles. Responding to concerns about target localization and potential mechanism-based side effects, an initial effort was also made to improve liver concentration in an available rat PK model. An advanced compound **17m** with a 5-carboxy-2-thiazole substructure appended to the spirocyclic piperidine scaffold was developed which satisfied the in vitro and in vivo requirements for more detailed studies.

Stearoyl-coenzyme A (CoA) desaturase (SCD) is involved in the de novo synthesis of monounsaturated fats from saturated fatty acids.[1] The major products of SCD are palmitoleoyl-CoA and oleoyl-CoA, which are formed by desaturation of palmitoyl-CoA and stearoyl-CoA, respectively. Oleate (an 18:1 fatty acid) is found to be the major monounsaturated fatty acid of membrane phospholipids, triglycerides, cholesteryl esters, wax esters and alkyl-1,2-diacylglycerol.[2] The ratio of unsaturated to saturated fatty acids is one of the factors influencing membrane fluidity; its alteration is important in a number of diseases, such as cancer, diabetes, obesity, and neurological, vascular and heart disease.[3–6] This ratio, referred to as the desaturation index, can be analyzed for multiple fatty acids in plasma including 18- and 16-carbon fatty acids, and represents a potential biomarker of SCD1 inhibition.

Depending on the species, highly homologous isoforms of SCD exist, differing primarily in tissue distribution.[7,8] For instance, in mice, four SCD isoforms have been identified, while two SCD isoforms have been found in humans, SCD1 and SCD5. In humans, adipose and liver tissues show the highest expression of SCD1, while brain and pancreatic tissues show highest expression of SCD5.[9] The overall sequence identity between human SCD1 and SCD5 is 61%.

In vivo studies in mice support the central role of SCD in both fatty acid metabolism and metabolic disorders. Mice strains with a naturally occurring mutation in one of the SCD isoforms (SCD1) and which have a targeted disruption in the SCD1 gene show reduced fatty acid and triglyceride synthesis in response to a high carbohydrate diet as compared to the amounts in wild type mice.[10] Furthermore, mice which have a targeted disruption in the SCD1 gene show reduced body adiposity, increased insulin sensitivity and resistance to diet-induced obesity.[11] Mice which were injected intraperitoneally with SCD1 targeted antisense oligonucleotide showed improved insulin sensitivity and prevented occurrence of obesity in the mice in response to high fat diets. In view of the experimental evidence described above, modulation of SCD represents a promising therapeutic strategy for the treatment of obesity and related metabolic disorders. However, given the wide distribution of SCD isoforms and their role in the fundamental process of fatty acid desaturation, there have also been concerns over possible mechanism-based side effects. Several companies have pursued programs based on SCD1 inhibitors (Fig. 1).[12–17] The major adverse effects reported for some of the compounds were alopecia and

* Corresponding author. Present address: Merck Research Laboratories, 33 Avenue Louis Pasteur, Boston, MA 02115, United States. Tel.: +1 617 992 3182.
E-mail address: yongqi.deng@merck.com (Y. Deng).
† Current address: Invitrogen Corporation, 4979 Smith Canyon Court, San Diego, CA 92130, United States.
‡ Current address: The New Venture Fund, Stoneham, MA 02180, United States.
§ Current address: Angiochem, 201 du Président-Kennedy, Montreal, QC, Canada H2X 3Y7.

0960-894X/$ - see front matter © 2012 Elsevier Ltd. All rights reserved.
http://dx.doi.org/10.1016/j.bmcl.2012.11.075

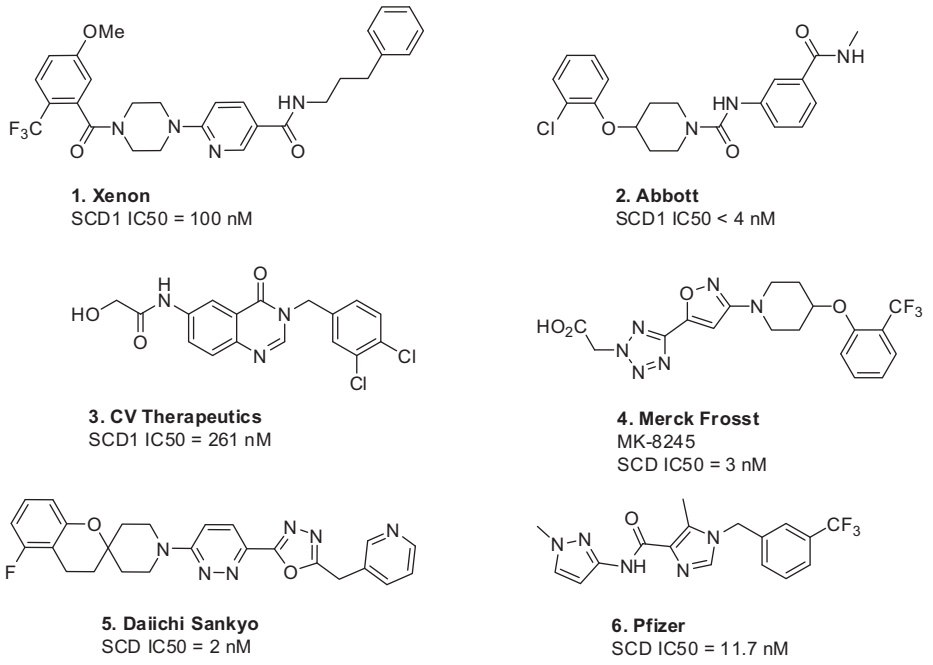

Figure 1. Recent published small molecule-based SCD1 inhibitors.

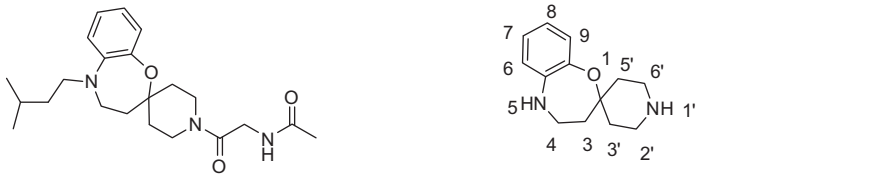

Figure 2. Initial HTS hit compound **7**.

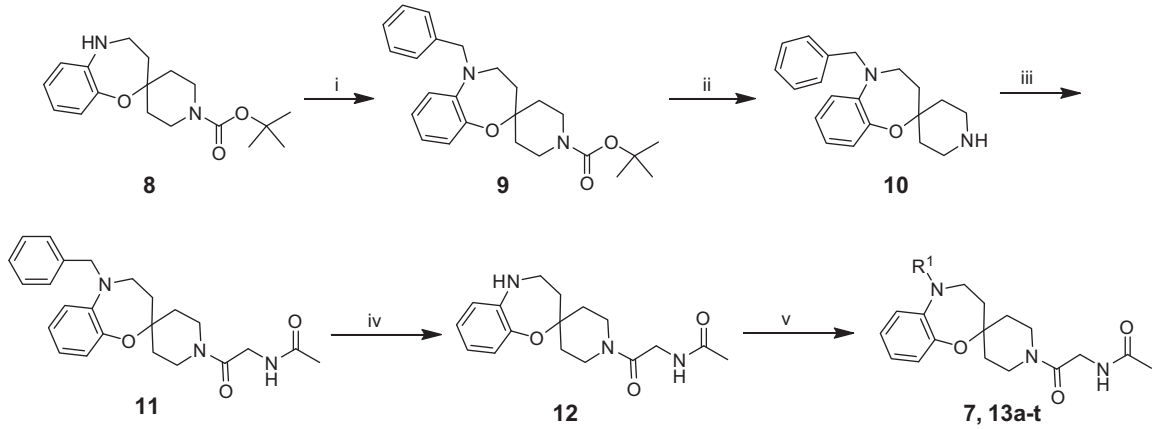

Scheme 1. Reagents and conditions: (i) benzaldehyde, $NaBH(AcO)_3$, acetonitrile, 50 °C, 85%; (ii) HCl in dioxane (4 N), rt, 0.5 h, 95%; (iii) 2-acetamidoacetic acid, HATU, DIEA, rt, 4 h, 70%; (iv) H_2, Pd/C (10%) rt, 12 h, 100%; (v) R_1CHO, $NaBH(AcO)_3$, acetonitrile, 50 °C or R_1Br, Cs_2CO_3.

partial eye closure.[18–21] The severity and the time at which these adverse effects were observed were directly related to the dose being administered, thus suggesting that the toxicity is related to the inhibitor's mechanism of action.

To overcome some of the side effects observed in the previous studies, one approach was to develop a SCD1 inhibitor with preferential distribution in liver tissue versus plasma and other tissues. With higher exposure at the targeted tissue, a wider therapeutic window was anticipated. Although there are several publications reporting this approach,[15,22] there are limited numbers of liver-targeted SCD1 inhibitors available in the literature. Herein, we report on a series of SCD1 inhibitors developed utilizing this

Table 1
Structure–activity relationships of SCD1 inhibitors at R^1

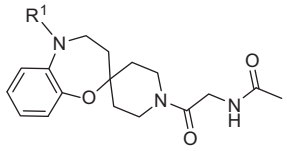

Compd	R^1	SCD1 IC_{50} (μM)
11	$PhCH_2$	1.2
13a	*iso*-Butyl	>10
13b	Propyl	>10
13c	Ph	>10
13d	$PhCH_2CH_2$	1.6
13e	2-$FPhCH_2$	>10
13f	2-Cl $PhCH_2$	1.2
13g	2-$MePhCH_2$	1.2
13h	2-$EtPhCH_2$	0.43
13i	2-$MeOPhCH_2$	2.9
13j	3-$FPhCH_2$	>10
13k	3-Cl $PhCH_2$	0.83
13l	3-MeO $PhCH_2$	1.8
13m	3-$F_3COPhCH_2$	0.68
13n	3-CF_3 $PhCH_2$	0.032
13o	4-$FPhCH_2$	0.46
13p	4-$ClPhCH_2$	>10
13q	4-$MePhCH_2$	1.1
13r	4-$EthylPhCH_2$	0.057
13s	4-*i*$PrPhCH_2CH_2$	0.042
13t	4-*t*$BuPhCH_2$	0.017

approach, and the in vitro and in vivo studies using a selection of these compounds.

A high throughput screen was developed to measure the inhibition of SCD1 in vitro.[23] Of the several series that were identified, the benzo-fused spirocyclic oxazepine scaffold (Fig. 2) appeared to have the most favorable combination of activity, preliminary SAR, and freedom to operate. By mining our internal collection, we were able to identify additional active compounds and generate broader potency patterns.

Compound **7** and its derivatives **11**, **13a–t** were synthesized following Scheme 1. The advanced intermediate Boc protected 4,5-dihydro-3*H*-spiro[1,5-benzoxazepine-2,4′-piperidine] **8** was prepared using literature procedures.[24] The 5-nitrogen of compound **8** was protected by a benzyl group by reacting it with benzaldehyde under reductive amination conditions to give compound **9**. Removing the Boc group of **9** with TFA afforded **10** and coupling it with acetyl glycine mediated by HATU in DMF gave **11** in good yield. To enable diversification at the 5-position of the 4,5-dihydro-3*H*-spiro[1,5-benzoxazepine-2,4′-piperidine] core, the benzyl protecting group of **11** was removed using catalytic hydrogenation to give compound **12**. Its derivatives were then subsequently synthesized under reductive amination, alkylation or arylation conditions.

Table 1 summarizes the SAR at the 5-position of the 4,5-dihydro-3*H*-spiro[1,5-benzoxazepine-2,4′-piperidine] core. Changing the isopentyl group of the progenitor **7** to smaller groups such as isobutyl and propyl moieties resulted in loss of potency (**13a** and **13b**). A direct linked phenyl group was also not tolerated (**13c**). However, a benzyl group showed improved potency (**11**) compared to **7**. Further extension of the linkage to two carbons gives a similar result as **13d** and demonstrated comparable potency to **11**. With these results in hand we decided to focus on modifications to the benzyl group.

The substitution on the benzyl group had profound effects on the inhibitory potency of the compounds. At the 2-position of the benzyl group, substituting hydrogen with fluoride (**13e**) resulted in loss of potency, but chloride (**13f**) maintained similar potency. While a methyl group (**13g**) retained similar potency, an ethyl group (**13h**) improved the potency by threefold. Although the methoxy group of **13i** bears the same number of atoms as the ethyl group, it reduced the potency by twofold, indicating that electronic effects were also important to the binding of the inhibitor to the enzyme. At the 3-position of the benzyl group replacement of the hydrogen with a fluorine (**13j**) was not tolerated, however a chlorine substituent (**13k**) improved potency. The electron rich methoxy group showed no impact on potency (**13l**) but the electron deficient trifluoromethoxy (**13m**) group improved the potency by twofold. Subsequently, a more electron withdrawing trifluoromethyl group was introduced and the potency improved by 40-fold (**13n**). Substitution at the 4-position displayed different SAR trends, for example devoid of activity. The impact of hydrophobicity at the 4-position was also evident; as changing from a methyl group to a *t*-butyl group boosted the potency from 1.1 to 0.017 μM (**13q**, **13r**, **13s** and **13t**).

With the identification of optimized motifs at the 5-position, we shifted our efforts to the optimization of the 1′-position. As shown in Scheme 2, the optimal R^1 was installed by reacting **8** with corresponding aldehydes under reductive amination condition to afford **14**, which was de-protected with TFA to give **15**. Subsquetnly, the compounds (**16a–m**) with various R^2 group at 1′-position were synthesized by reacting **15** with corresponding carboxylic acids and the bioactivities of this set of compounds are listed in Table 2. Relative to **13q**, substitution at the α carbon was not tolerated as both **16a** and **16b** lost their inhibitory activities. Replacing the acetamide with a benzamide (**16c**) or nicotinamide (**16e**) resulted in significant loss of potency, while the 2-furancarboxamide (**16f**) restored potency. In comparing different amide substitents, 4-*tert*-butylbenzyl showed better compatibility than the 3-trifluoromethylbenzyl groups at the 5-position of the core, as **16c** and **16f** exhibited better potency relative to the corresponding compounds **16d** and **16g**. Further optimization efforts resulted in little progress towards additional potency improvement (**16h–n**).

Examination of the structures of other reported inhibitors[25] revealed that heterocycles, particularly pyridazine, had been used to link an amide to the core and shown activity enhancement. To incorporate this motif into our series of inhibitors 6-bromo-*N*-(2-cyclopropylethyl)-pyridazine-3-carboxamide was used to react with the intermediate **15a** and **15b** under a thermal condition to afford the corresponding compounds **17a** and **17b** (Scheme 3).

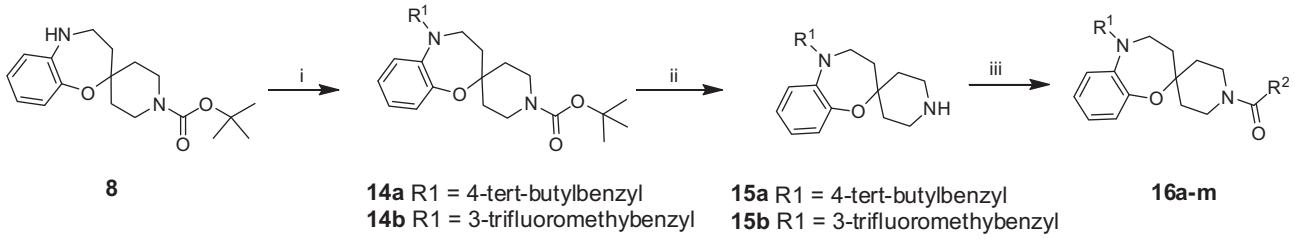

Scheme 2. Reagents and conditions: (i) 4-*tert*-butylbenzaldehyde or 3-trifluoromethybenzaldyde, $NaBH(AcO)_3$, acetonitrile, 50 °C, 85%; (ii) HCl in dioxane (4 N), rt, 0.5 h, 90%; (iii) R_2COOH, HATU, DIEA, rt, 4 h, 70%.

Table 2
Structure–activity relationships of SCD1 inhibitors at R^2

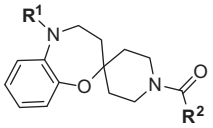

Compd	R^2	R^1	SCD1 IC_{50} (μM)
16a	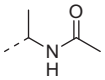	4-*t*BuPhCH$_2$	>10
16b	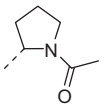	4-*t*BuPhCH$_2$	>10
16c	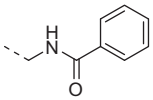	4-*t*BuPhCH$_2$	0.35
16d	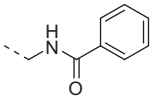	3-CF_3PhCH$_2$	2.6
16e	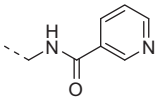	4-tBuPhCH$_2$	1.5
16f	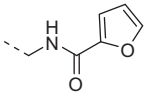	4-tBuPhCH$_2$	0.019
16g	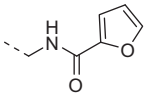	3-CF_3PhCH$_2$	0.38
16h	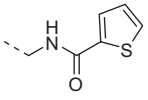	4-tBuPhCH$_2$	0.14
16i	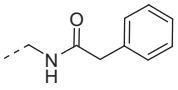	4-tBuPhCH$_2$	8.2
16j	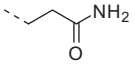	4-tBuPhCH$_2$	0.18
16k	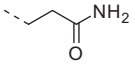	3-CF_3PhCH$_2$	2.45
16l	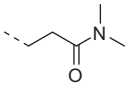	4-tBuPhCH$_2$	5.9
16m		4-tBuPhCH$_2$	0.44
16n	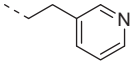	4-tBuPhCH$_2$	3.3

Table 3
Structure–activity relationships of SCD1 inhibitors at R^3

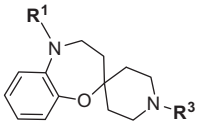

C0mpd	R^1	R^3	SCD1 IC_{50} (μM)
17a	4-*t*BuPhCH$_2$	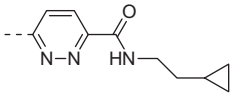	0.04
17b	3-CF_3PhCH$_2$	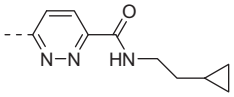	0.004
17c	3-CF_3PhCH$_2$	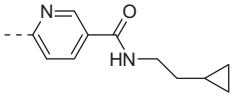	0.012
17d	3-CF_3PhCH$_2$	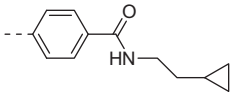	2.2
17e	3-CF_3PhCH$_2$	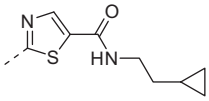	0.93
17f	3-CF_3PhCH$_2$	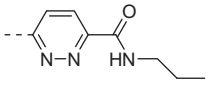	0.13
17g	3-CF_3PhCH$_2$	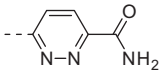	0.01
17h	3-CF_3PhCH$_2$	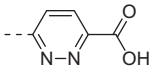	4.7
17i	3-CF_3PhCH$_2$	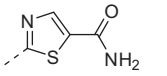	0.003
17j	3-CF_3PhCH$_2$	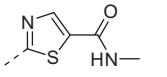	0.003
17k	4-*t*BuPhCH$_2$	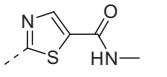	0.004
17l	3-CF_3PhCH$_2$	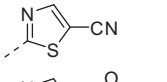	0.001
17m	3-CF_3PhCH$_2$	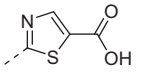	0.008

We were pleased to find that both compounds showed good inhibitory potency and interestingly, 3-trifluoromethylbenzyl substituents at the 5-position of the core gave 10-fold better potency compared to a 4-*tert*-butylbenzyl group (Table 3). The large

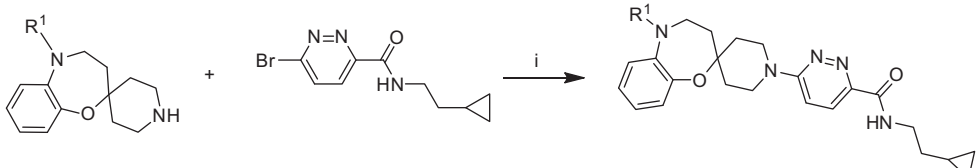

15a R1 = 4-tert-butylbenzyl
15b R1 = 3-trifluoromethybenzyl

17a R1 = 4-tert-butylbenzyl
17b R1 = 3-trifluoromethybenzyl

Scheme 3. Reagents and conditions: (i) DIEA, micro wave, 120 °C, 10 min, 65%

Table 4
Pharmacokinetic data of selected compounds

Compd	AUC (ng/g h)	C_{max} (ng/g)	Plasma C6h (ng/g)	Liver C6h (ng/g)	C6h liver/plasma
13r	1288	579	19	<100	n/a
13s	2608	875	100	1655	17
13t	3464	1095	210	2673	13
16e	341	169	18	232	13
17b	105	209	0	<10	n/a
17c	23	45	0	<10	n/a
17i	58	45	0	<10	n/a
17j	0	0	0	0	n/a
17l	383	105	72	1509	20
17m	2308	495	345	19,246	56
2	1435	599	66	529	8.0

substitute on the amide was preferred as **17f** and **17g** were less active. Since it is known that pyridazine amides can potentially be subjected to extensive metabolism, [26] other heterocycles were also explored. Replacing pyridazine with a pyridine group (**17c**) reduced potency slightly, while replacing it with a phenyl group (**17d**) diminished the potency to above 1 μM. The thiazole derivatives showed distinct SAR as the initial thiazole replacement gave a compound with reduced potency (**17e**), but its smaller amide derivatives exhibited more favorable inhibition of SCD1 (**17i**, **17j, 17k**). Also, its cyano derivative **17l** showed comparable potency relative to its corresponding amide. As carboxylic acid derivatives are potentially capable of distributing into the liver tissue preferentially, several carboxylic acids were prepared. In contrast to the low potency of pyridazine carboxylic acid **17h**, the thiazole carboxylic acid derivative **17m** demonstrated excellent potency.

Several potent compounds from different subseries were selected to dose at 10 mg/kg in rats to evaluate their pharmacokinetic profiles. In addition to the drug exposure in plasma, drug concentration in brain and liver was also recorded at the 6 h time point; the data is summarized in Table 4. Among the compounds evaluated, **17m** displayed a desired pharmacokinetic profile. This compound shows moderate exposure in plasma (AUC = 4.1 μg/g h) and has been found to target liver tissue preferentially. At 6 h post dosing, the liver concentration was 21.7 μg/g versus 0.46 μg/g in plasma, resulting in a liver/plasma ratio of 47. Due to its potent enzymatic activity and superior PK properties, we decided to conduct further in vivo studies using **17m**.

Compound **17m** was evaluated in an acute efficacy study using AKR mice, along with a control compound **2** (Fig. 3).[13] Both compounds were dosed 4 h before plasma sample collection. Table 5 lists the concentration of **17m** and **2** in plasma samples. To measure the in vivo SCD-1 activity, a desaturation index was calculated from ratios of 16:1/16:0 or 18:1/18:0 fatty acids. Figure 3 shows the lowering effect on the desaturation index following treatment with **17m** and **2**. A dose-dependent desaturation index reduction by **17m** was observed, with a 21% reduction at 30 mg/kg, as measured by both 16:1/16:0 and 18:1/18:0. The control compound **2** showed 16% reduction in the desaturation index using 16:1/16:0 ratio and 22% reduction using 18:1/18:0 ratio when dosed at 30 mg/kg.

Table 5
Concentration (ng/mL) of **17m** and **2** in plasma collected at 4 h after dosing

Dose	1 mg/kg	3 mg/kg	10 mg/kg	30 mg/kg
17m	0.64	45	135	1742
2				1775

In the preliminary analysis, no abnormalities were observed in the skin or eyes of the mice dosed at 30 mg/kg. The potential toxicity of **17m** was assessed in male CD-1 mice administered single daily doses of 0, 30, 100 or 300 mg/kg by oral gavage **17m** and 300 mg/kg **2** for 2 weeks. All animals survived to terminal necropsy with no effects on body weight or food consumption. Clinical signs for mice administered **17m** were limited to a few instances of lacrimation in the 300 mg/kg dose group. Clinical signs for mice administered **2** consisted of peri-orbital swelling, alopecia, ocular opacity, swelling of the lips and lacrimation in the 300 mg/kg dose group.

There were no **17m** or **2**-related changes in hematology or serum chemistry parameters. Small testes were observed in 3 of 4 mice in the 300 mg/kg **17m** dose group at terminal necropsy. Mean absolute and relative liver weights were higher in the 100 mg/kg (19% and 20%, respectively) and 300 mg/kg (29% and 33%, respectively) dose groups, compared to controls. Absolute and relative peri-renal fat weights were lower than controls (not dose-related) for the 100–300 mg/kg **17m** dose groups and the 300 mg/kg **2** dose group. Peri-renal fat weights for the 100 mg/kg **17m** dose group were comparable to the 300 mg/kg **2** dose group.

Compound **17m** and **2** related microscopic findings were seen in the harderian gland (atrophy, hyperplasia), skin (atrophy of sebaceous gland), eyelid (atrophy of sebaceous gland), meibomian gland (atrophy, squamous metaplasia) and eyes (corneal degeneration, inflammation). Atrophy of the harderian and meibomian glands were observed in all dose groups. Changes in the eyes were considered secondary to atrophy of the harderian glands. The microscopic changes in the 300 mg/kg **17m** dose group were comparable to the findings for the 300 mg/kg **2** dose group. Dose-related tubular atrophy of the testes was observed in the

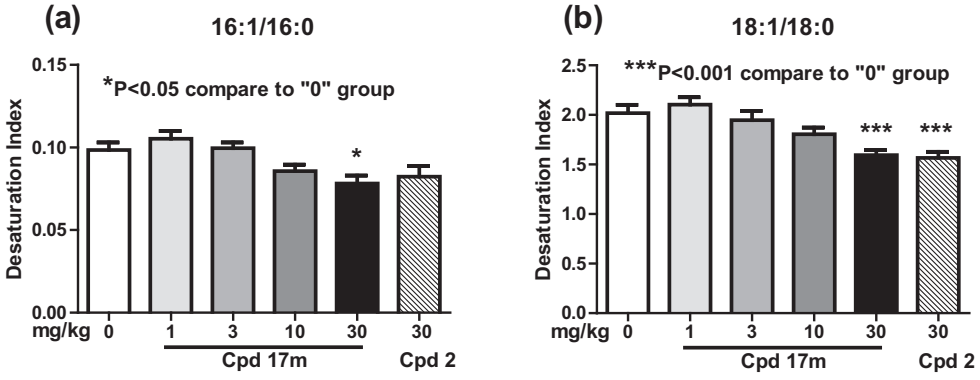

Figure 3. Plasma desaturation index lowering effect of SCD1 inhibitor **17m** and **2** after 4 h treatment in 7 week old male AKR/J mice (n = 10/group) fed a 10% Kcal low fat diet (Research Diets, D12450B). (a) Plasma desaturation index derives from fatty acids 16:1/16:0 and (b) plasma desaturation index derives from fatty acids 18:1/18:0.

100–300 mg/kg groups. Minimal Leydig cell hyperplasia of the testes was seen only in the 300 mg/kg **17m** dose group. There were no test-article related testes findings for the **2** group.

Plasma-drug levels were determined at Day 13 following 2 weeks of daily dosing. Dose-related increases for both exposure and C_{max} were observed for **17m**. Exposure [AUC(0–24 h)] for **17m** at 30, 100 and 300 mg/kg was 114, 565 and 1520 μM h, respectively. Exposure [AUC (0–24 h)] for **2** at 300 mg/kg was 216 μM h. Low levels of the glucuronide conjugate metabolite were observed for **17m** in the 300 mg/kg samples.

Compound **17m** administered orally for 2 weeks at doses of 30, 100 and 300 mg/kg caused stearoyl-CoA desaturase inhibitor class effects similar to **2** (i.e., inhibition of fatty acid metabolism leading to lesions of the eye and skin). Microscopic findings were comparable between **17m** and **2**, despite greater dose-related exposure to **17m**. Further evaluation would be required to understand testicular effects observed with **17m**.

In conclusion, we have identified a highly potent SCD1 inhibitor **17m** with excellent pharmacokinetic profiles and a favorable tissue distribution profile. As for the in vivo evaluation, **17m** showed moderate reduction of the desaturation index in the plasma after a 4 h oral administration at 30 mg/kg. Although no notable abnormalities in the eyes or skin were observed at this dose, studies with higher dosages over an extended period generated side effects related to target inhibition, suggesting further enhancement of the selective distribution into the liver may be necessary to reduce side effects and to develop this series of SCD1 inhibitors for the treatment of metabolic disorders.

References and notes

1. Ntambi, J. M. *J. Lipid Res.* **1999**, *40*, 1549.
2. Miyazaki, M.; Ntambi, J. M. *Prostaglandins Leukot. Essent.* **2003**, *68*, 113.
3. Spiegelman, B. M.; Choy, L.; Hotamisligil, G. S.; Graves, R. A.; Tontonoz, P. *J. Biol. Chem.* **1993**, *268*, 6823.
4. Storlien, L. H.; Jenkins, A. B.; Chisholm, D. J.; Pascoe, W. S.; Khouri, S.; Kraegen, E. W. *Diabetes* **1991**, *40*, 280.
5. Solans, R.; Motta, C.; Sola, R.; La Ville, A. E.; Lima, J.; Simeon, P.; Montella, N.; Armadans-Gil, L.; Fonollosa, V.; Vilardell, M. *Arthritis Rheum.* **2000**, *43*, 894.
6. Agatha, G.; Hafer, R.; Zintl, F. *Cancer Lett.* **2001**, *173*, 139.
7. Ntambi, J. M.; Miyazaki, M. *Curr. Opin. Lipidol.* **2003**, *14*, 255.
8. Miyazaki, M.; Jacobson, M. J.; Man, W. C.; Cohen, P.; Asilmaz, E.; Friedman, J. M.; Ntambi, J. M. *J. Biol. Chem.* **2003**, *278*, 33904.
9. Flowers, M. T.; Ntambi, J. M. *Curr. Opin. Lipidol.* **2008**, *19*, 248.
10. Miyazaki, M.; Flowers, M. T.; Sampath, H.; Chu, K.; Otzelberger, C.; Liu, X.; Ntambi, J. M. *Cell Metab.* **2007**, *6*, 484.
11. Ntambi, J. M.; Miyazaki, M. *Curr. Opin. Lipidol.* **2003**, *14*, 255.
12. Fu, J. -M.; Kodumuru, V., Sun, S., et al. Nicotinamide derivatives and their use as therapeutic agents. US20050119251; 2005.
13. Xin, Z. L.; Zhao, H. Y.; Serby, M. D.; Liu, B.; Liu, M.; Szczepankiewicz, B. G.; Nelson, L. T. J.; Smith, H. T.; Suhar, T. S.; Janis, R. S.; Cao, N.; Camp, H. S.; Collins, C. A.; Sham, H. L.; Surowy, T. K.; Liu, G. *Bioorg. Med. Chem. Lett.* **2008**, *18*, 4298.
14. Koltun, D. O.; Vasilevich, N. I.; Parkhill, E. Q.; Glushkov, A. I.; Zilbershtein, T. M.; Mayboroda, E. I.; Boze, M. A.; Cole, A. G.; Henderson, I.; Zautke, N. A.; Brunn, S. A.; Chu, N.; Hao, J.; Mollova, N.; Leung, K.; Chisholm, J. W.; Zablocki, J. *Bioorg. Med. Chem. Lett.* **2009**, *19*, 3050.
15. Oballa, R. M.; Belair, L.; Black, W. C.; Bleasby, K.; Chan, C. C.; Desroches, C.; Du, X. B.; Gordon, R.; Guay, J.; Guiral, S.; Hafey, M. J.; Hamelin, E.; Huang, Z.; Kennedy, B.; Lachance, N.; Landry, F.; Li, C. S.; Mancini, J.; Normandin, D.; Pocai, A.; Powell, D. A.; Ramtohul, Y. K.; Skorey, K.; Sorensen, D.; Sturkenboom, W.; Styhler, A.; Waddleton, D. M.; Wang, H.; Wong, S.; Xu, L. J.; Zhang, L. *J. Med. Chem.* **2011**, *54*, 5082.
16. Uto, Y.; Ueno, Y.; Kiyotsuka, Y.; Miyazawa, Y.; Kurata, H.; Ogata, T.; Yamada, M.; Deguchi, T.; Konishi, M.; Takagi, T.; Wakimoto, S.; Ohsumi, J. *Eur. Med. Chem.* **2010**, *45*, 4788.
17. Atkinson, K. A.; Beretta, E. E.; Brown, J. A.; Castrodad, M.; Chen, Y.; Cosgrove, J. M.; Du, P.; Litchfield, J.; Makowski, M.; Martin, K.; McLellan, T. J.; Neagu, C.; Perry, D. A.; Piotrowski, D. W.; Steppan, C. M.; Trilles, R. *Bioorg. Med. Chem. Lett.* **2011**, *21*, 1621.
18. Nakamura, M. T.; Nara, T. Y. *Annu. Rev. Nutr.* **2004**, *24*, 345.
19. Miyazaki, M.; Kim, Y. C.; Gray-Keller, M. P.; Attie, A. D.; Ntambi, J. M. *J. Biol. Chem.* **2000**, *275*, 30132.
20. Li, C. S.; Belair, L.; Guay, J.; Murgasva, R.; Sturkenboom, W.; Ramtohul, Y. K.; Zhang, L.; Huang, Z. *Bioorg. Med. Chem. Lett.* **2009**, *19*, 5214.
21. Leger, S.; Black, W. C.; Deschenes, D.; Dolman, S.; Falgueyret, J. P.; Gagnon, M.; Guiral, S.; Huang, Z.; Guay, J.; Leblanc, Y.; Li, C. S.; Masse, F.; Oballa, R.; Zhang, L. *Bioorg. Med. Chem. Lett.* **2010**, *20*, 499.
22. Lachance, N.; Gareau, Y.; Guiral, S.; Huang, Z.; Isabel, E.; Leclerc, J. P.; Leger, S.; Martins, E.; Nadeau, C.; Oballa, R. M.; Ouellet, S. G.; Powell, D. A.; Ramtohul, Y. K.; Tranmer, G. K.; Trinh, T.; Wang, H.; Zhang, L. *Bioorg. Med. Chem. Lett.* **2012**, *22*, 980.
23. Leger, S.; Black, W. C.; Deschenes, D.; Dolman, S.; Falgueyret, J. P.; Gagnon, M.; Guiral, S.; Huang, Z.; Guay, J.; Leblanc, Y.; Li, C. S.; Masse, F.; Oballa, R.; Zhang, L. *Bioorg. Med. Chem. Lett.* **2010**, *20*, 499. detailed procedure as following: in 100 μl of 100 mM Tris HCl, pH 7.3/2 mM NADH/20 μM stearoyl-CoA containing 0.75 μCi [9,10-3*H*-stearoyl] stearoyl-CoA per well. After a 15-min incubation at room temperature, plates were transferred to ice and 10 μl of 20% trichloroacetic acid was added to each well. After 5 min on ice, a 90-μl volume from each well was transferred to a Millipore Multiscreen HTS 96-well filtration plate, the wells of which contained 125 μl of 10% activated charcoal to which vacuum had been previously applied to remove excess liquid and a plastic seal then applied to the bottom. Plates were shaken 15 min and the contents were then filtered into a 96-well collection plate. A 50-μl volume of filtrate was counted in 150 μl of MicroScint 40 in a TopCount scintillation counter. Stock solutions of compounds, 10 mM in DMSO, were diluted in DMSO for a final assay concentration of 2% DMSO. Percent inhibition was determined as (total-sample)/(total-blank)(100); total activity was determined in the presence of 2% DMSO and blank in the presence of 10–4 M concentration of a standard inhibitor in 2% DMSO. The inhibition constant was determined with the Prism non-linear, least-squares, curve-fitting program.
24. Miyazaki, M.; Man, W. C.; Ntambi, J. M. *J. Nutr.* **2001**, *131*, 2260.
25. Leger, S.; Black, W. C.; Deschenes, D.; Dolman, S.; Falgueyret, J. P.; Gagnon, M.; Guiral, S.; Huang, Z.; Guay, J.; Leblanc, Y.; Li, C. S.; Masse, F.; Oballa, R.; Zhang, L. *Bioorg. Med. Chem. Lett.* **2010**, *20*, 499.
26. Uto, Y.; Ogata, T.; Kiyotsuka, Y.; Miyazawa, Y.; Ueno, Y.; Kurata, H.; Deguchi, T.; Yamada, M.; Watanabe, N.; Takagi, T.; Wakimoto, S.; Okuyama, R.; Konishi, M.; Kurikawa, N.; Kono, K.; Osumi, J. *Bioorg. Med. Chem. Lett.* **2009**, *19*, 4159.